

Effect of the Depth of the Solution Layer on the Atmospheric Corrosion of Carbon Steel

M.E. Escalante-Perez^{1,2}, J. Porcayo-Calderon^{1,*}, E. Vazquez-Velez², M. Casales-Diaz²,
J.G. Gonzalez-Rodriguez¹, L. Martinez-Gomez^{2,3}

¹ Universidad Autonoma del Estado de Morelos, CIICAp, Av. Universidad 1001, 62209-Cuernavaca, Morelos, Mexico

² Universidad Nacional Autonoma de Mexico, Instituto de Ciencias Fisicas, Av. Universidad s/n, Cuernavaca, Morelos, Mexico

³ Corrosion y Proteccion, Buffon 46, Mexico City, C.P. 11590, Mexico

*E-mail: jporcayoc@gmail.com

Received: 5 October 2015 / *Accepted:* 17 November 2015 / *Published:* 1 December 2015

Atmospheric corrosion occurs under alternate cycles in presence and absence of an electrolyte layer, the severity of corrosion processes that occur onto the metallic surface depends largely on the corrosive environment to which the material is exposed. Whereas the corrosive phenomena occur in the presence of the electrolyte, in this work the effect of the depth of the solution layer on the electrochemical behavior of carbon steel was determined. Three different corrosive media were employed to simulate the effect of coastal and rural environments. The results showed a strong dependence of the corrosion rate of carbon steel with the depth of the solution layer. Corrosive events on the material are governed by diffusion processes of species from the bulk solution to the steel surface.

Keywords: atmospheric corrosion, depth of the solution layer, electrochemical techniques.

1. INTRODUCTION

Metallic corrosion in atmospheric environments is significantly different from that which occurs into bulk solution [1]. Atmospheric corrosion can be defined as wet corrosion, and it occurs when the metallic surface is under the influence of a thin layer of electrolyte. Notwithstanding this, in these conditions also apply the general laws that governing the electrochemical corrosion of metals immersed in an electrolyte [2]. It is known that the thickness of the electrolyte layer plays an important role in the corrosion behavior of a metal [1]. It has been reported that the variation in the thickness of

the electrolyte layer influences some processes such as; the limiting current density of oxygen reduction, accumulation of corrosion products and the hydration of dissolved metal ions [3].

Similarly, it has been reported that for electrolyte layers with thickness between 10-100 microns, the corrosion is controlled by cathodic processes, where the transport of dissolved oxygen is inversely proportional to the diffusion layer thickness. For electrolyte thicknesses layer near to 10 microns, the oxygen transfer across the air/solution interface is the rate limiting, and for electrolyte thicknesses layer near to 100 microns the convection controls the diffusion layer thickness [4]. Furthermore, the anodic reaction rate decreases with decreasing the thickness of the electrolyte layer, because the solubility of the reaction products decreases [5-8]. On the other hand, the type of attack and the corrosion rate directly dependent on the environment to which the materials are exposed. Even pure water can corrode to the metallic materials in the presence of dissolved oxygen [9].

Generally speaking, the corrosion can occur from extremely thin electrolyte layers and droplets covering the metallic surface exposed to humidity cycles to industrial structures immersed in voluminous corrosive environments. Corrosion studies in either extremely thin electrolyte films and droplets have been conducted to determine the factors that initiate the metallic corrosion in atmospheric environments [1, 2, 4, 10-14]. However, many studies about atmospheric corrosion are also performed in conditions of total immersion, but in most cases it is not specified the depth of the solution layer existing onto surface of the tested materials. Therefore, the idea of this work is to determine the effect of the depth of the solution layer on the electrochemical response of the carbon steel immersed in various corrosive environments under static conditions.

2. EXPERIMENTAL PROCEDURE

Corrosion tests were realized on 1018 carbon steel samples. The test specimens were cut into small parallelepiped pieces of 10.0 x 10.0 x 3.0 mm. For electrical connection, specimens were spot-welded to a Cu wire, and then mounted and encapsulated in thermosetting resin. Sample surfaces were ground to 600 grade grit paper, then rinsed with distilled water and later by ethanol in an ultrasonic bath for 10 minutes. Specimens with this surface condition were employed as the working electrode (WE) in the electrochemical tests.

Three types of solutions were used in order to simulate different atmospheric environments; distilled water, 0.01 M Na_2SO_4 solution for rural atmospheres, and a (0.5 g/l NaCl + 3.5 g/l $(\text{NH}_4)_2\text{SO}_4$) solution for marine atmospheres. In order to evaluate the effect of the depth of the solution layer, an electrochemical cell as illustrated in Figure 1 was employed, where "d" is the average depth of the solution layer on the sample. Three different depths of the solution layer were evaluated, namely, 0.1 cm, 1.0 cm and 10.0 cm. The tests were conducted at room temperature and under static conditions.

Electrochemical tests were carried out using an ACM Instruments zero-resistance ammeter (ZRA) coupled to a personal computer. A typical three electrodes arrangement was used, the reference electrode (RE) was a saturated calomel electrode and the counter electrode (CE) was a platinum wire. All the potentials described in the text are relative to the SCE, unless stated differently. For each

electrochemical test a volume of 200 ml of fresh solution was used. Polarization curves were recorded at a constant sweep rate of 1 mV/s, and the scanning range was from -400 to $+700$ mV versus the open circuit potential. To assess the capability of the material to form a protective oxide scale on their surfaces upon immersion in the testing solution the free corrosion potential as a function of time of the working electrodes E_{corr} , was measured versus a SCE for 24 hours. Linear polarization curves were obtained by polarizing the specimens from -20 to 20 mV versus the free corrosion potential value, E_{corr} , at a scanning rate of 1 mV/s, measurements were made for 24 hours.

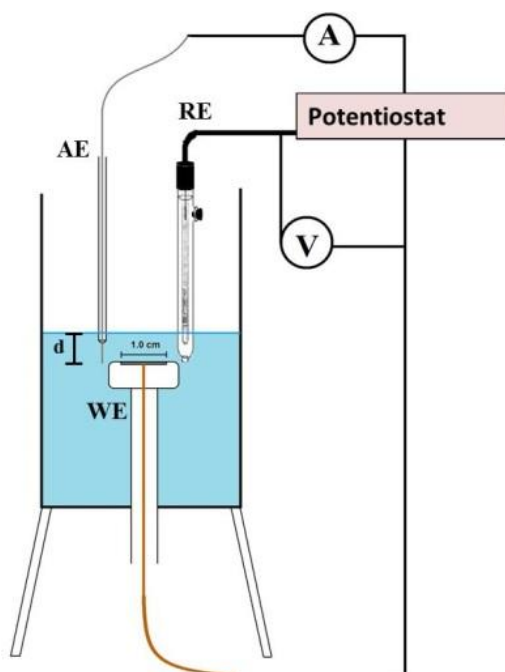


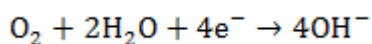
Figure 1. Experimental set-up for electrochemical measurements.

3. RESULTS AND DISCUSSION

3.1. Potentiodynamic Polarization Curves

Figure 2 shows the potentiodynamic polarization curves for 1018 carbon steel in distilled water. Polarization curves show that decreasing the depth of the solution layer, the E_{corr} values become more active. The anodic branch shows an active corrosion process, and the cathodic branch shows that by increasing the depth of the solution layer increases the cathodic current density.

It is said that in not deaerated systems the main cathodic reaction is the O_2 reduction reaction, and it is a multielectron reaction that includes a number of elementary steps involving different reaction intermediates [15]. In aqueous solutions at neutral or slightly alkaline pH the cathodic reaction is [16]:



Ec. 1

Where the rate determining step is the addition of the first electron to the oxygen dissolved [15]:



Further, it has been reported that an increase in the resistance of the O₂ diffusion, due to the build-up of the oxide layer, provokes a decrease in the limiting current density for O₂ reduction on the carbon steel surface [17]. It is therefore possible to say that the decrease in the cathodic current values by decreasing the depth of the solution layer it is due to the depletion of dissolved oxygen onto carbon steel surface, that is, the reduction reactions deplete the available oxygen, and its supply to the carbon steel surface is limited either by its absorption rate or diffusion. This may be related to the amount of available oxygen into the solution layer, ie, in a deeper solution layer (larger volume) the amount of oxygen available for the reduction reaction is greater. In the case of extremely thin electrolyte films a contrary behavior is observed, namely, cathodic current density increases by decreasing the thickness electrolyte film [4].

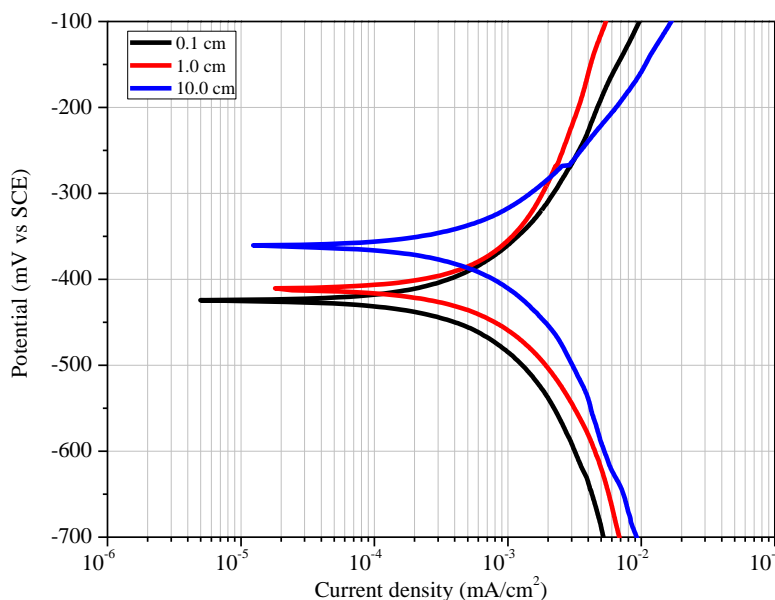


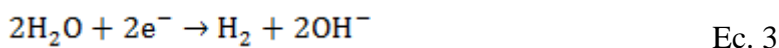
Figure 2. Potentiodynamic polarization curves for 1018 carbon steel in distilled water.

Figure 3 shows the polarization curves for the 1018 carbon steel evaluated in a simulated rural environment (0.01 M Na₂SO₄ solution). From figure a shift (around 120 mV) in the E_{corr} values can be observed by increasing one order of magnitude the depth of the solution layer. The E_{corr} values become active by reducing the depth of the solution layer. Although the slope of the anodic branches decreases by increasing the depth of the solution layer, the I_{corr} values do not vary appreciably. Furthermore, the anodic branches tend to converge to the same potential value (about -300 mV). On the other hand, the cathodic branches show the same shape and the same limit current. However, its length increases by increasing the depth of the solution layer. Similar cathodic branches have been reported [1, 12], and three main regions can be observed:

Region I. It corresponds to the region near to the corrosion potential. Its shape depends on the thickness of the depth of the solution layer. For 1.0 to 10 cm of depth of the solution, near to E_{corr} , the presence of perturbations can be observed, and this can be associated with the reduction of corrosion products formed during the stabilization period.

Region II. Beyond 50 mV from E_{corr} , the behavior it is attributed to the oxygen reduction controlled by mass transfer. In this region it takes place the reduction both oxygen and corrosion products, and it is controlled by the oxygen diffusion rate [18, 19]. The length of this zone decreases by decreasing the depth of the solution layer, this may indicate that the amount of reducible oxygen is proportional to the solution volume. That is, the depth of the solution layer acts as a reservoir of oxygen available for the cathodic reaction. However, the limited diffusion current is not affected by the depth of the solution layer.

Region III. Beyond -950mV, the cathodic current density rapidly increases because to the hydrogen evolution reaction:



The potential where hydrogen evolution begins is designated as E_{2H^+/H_2} . If $\Delta E = (E_{corr} - E_{2H^+/H_2})$, ΔE increases by increasing the depth of the solution layer. This suggests that the hydrogen reduction reaction begins once it has depleted the available oxygen in the electrolyte layer.

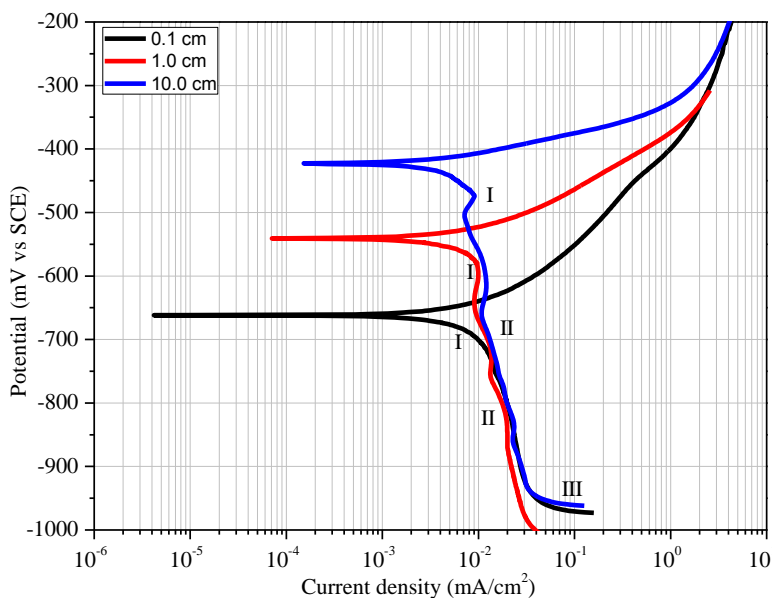


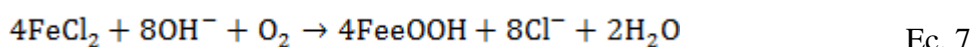
Figure 3. Potentiodynamic polarization curves for 1018 carbon steel in simulated rural environment.

Figure 4 shows the polarization curves for the 1018 carbon steel evaluated in a simulated marine environment (0.5 g/l NaCl + 3.5 g/l $(NH_4)_2SO_4$ solution). The anodic branch indicates an active corrosion process, where at very anodic potentials, the current density increases by increasing the depth of the solution layer. It is noted that the E_{corr} values depend on the depth of the solution layer,

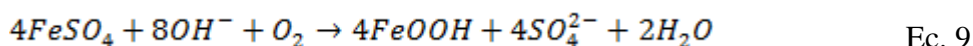
being than increasing the depth of the solution layer the E_{corr} value is nobler. From the cathodic branch is observed that the current density decreases by decreasing the depth of the solution layer. According to Zhang and Lyon [2], this can be due to the depletion of reactants. In the presence of $(NH_4)_2SO_4$ the cathodic behavior differs substantially from those observed in NaCl, due to different corrosion mechanisms. If the concentration of $(NH_4)_2SO_4$ is greater than that of NaCl, the cathodic behavior is due the following reduction reactions [20]:



Moreover, the NH_4^+ ions present have the ability to inhibit oxide film formation. In the presence of Cl^- ions, the following reactions occur:



And, in the presence of SO_4^{2-} ions, also the following reactions occur:



$FeCl_2$ and $FeSO_4$ are unstable corrosion products which can be reoxidized to $FeOOH$, and both SO_4^{2-} and Cl^- ions restart the corrosive cycle.

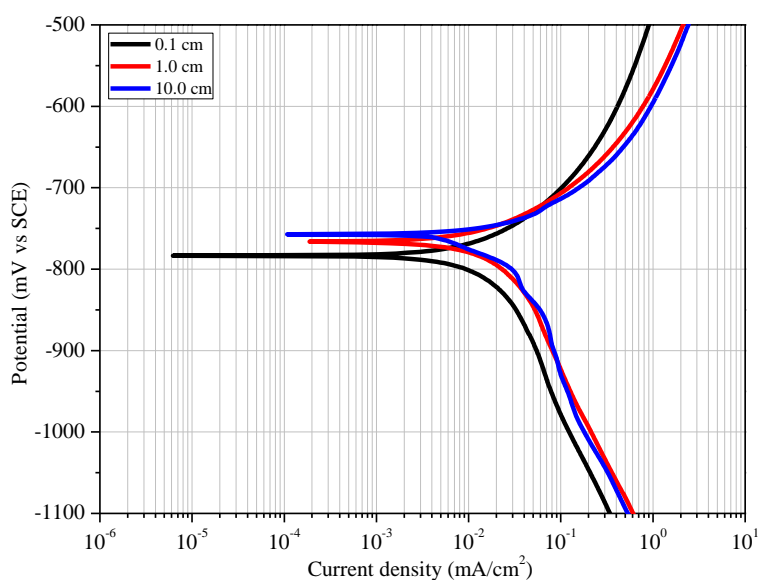


Figure 4. Potentiodynamic polarization curves for 1018 carbon steel in simulated marine environment.

In electrolytes where there are more than one species of ions, it is more complicated explaining the behavior of the materials. It is said that the aggressive behavior of chlorides and sulfates is synergistic. When the concentration of chloride is low, the sulfate ion is easily adsorbed to the metallic surface [21].

Table 1 shows the electrochemical parameters obtained from the previous figures. β_a and β_c are referred to as the Tafel slopes. Changes in the slope values can be associated with the surface processes occurring onto the working electrode. A large anodic slope indicates that the metal surface is easily polarized due to the rapid formation of a protective oxide layer onto electrode/electrolyte interface. If the cathodic slope is greater than the anodic slope, the cathodic reaction is the rate-limiting factor of the corrosion process, and it is being controlled by the transport of the active species toward the cathode [22-23]. If the cathodic slope is around 0.2V/decade, the corrosion process is not controlled by charge transfer reactions, otherwise the corrosion process is influenced by the supply of electroactive species to the electrode surface [24]. In particular, analyzing the values of the cathodic pending Table 1, it can be observed that both in distilled water and marine environments, decreasing the depth of the solution layer increases the value of the slope cathode which indicates that the corrosion process becomes controlled by the supply of Electroactive species to the electrode surface. The opposite occurs in marine environment, this may be because the main reduction reactions are different as mentioned above.

Table 1. Electrochemical parameters for carbon steel in simulated corrosive media.

Electrolyte	Depth	E _{corr}	β_a	β_c	I _{corr}
Distilled water	0.1 cm	-424.99	253.71	269.62	0.0007
	1.0 cm	-411.53	306.45	201.44	0.0006
	10.0 cm	-399.39	262.66	183.46	0.0007
Rural environment	0.1 cm	-662.02	126	405	0.009
	1.0 cm	-540.76	84.43	193.47	0.0059
	10.0 cm	-422.44	42.31	123.4	0.0036
Marine environment	0.1 cm	-784.44	106.3	214.26	0.016
	1.0 cm	-775.7	127.57	262.28	0.0252
	10.0 cm	-768.78	94.2	275.53	0.0186

3.2. Open Circuit Potential (OCP)

Figure 5 shows the effect of the depth of the solution layer on the open circuit potential for the carbon steel evaluated in different environments. In general, it observed that carbon steel showed drastic changes in their E_{corr} values throughout the corrosion test.

In distilled water, carbon steel showed the highest thermodynamic instability, the E_{corr} values tended steadily to more active values during the 24 hours of immersion. In general, a ΔE of 400 mV in the first 12 hours of immersion is observed, and subsequently the potential drop was slower. This behavior can be associated with a decrease in dissolved oxygen concentration available for the reduction reaction onto metallic surface [4, 17].

In rural simulated environment, for a depth of the solution layer of 0.1 cm, an E_{corr} drop in the first 8 hours of immersion was observed, and after that, a slight increase is observed as time evolved. Similar behavior is observed in a depth of the solution layer of 1.0 cm. However, for a depth of the solution layer of 10 cm, E_{corr} values constantly decrease during the 24 hour of test. It is noted that regardless of the depth of the solution layer, E_{corr} values tend around the same value.

In simulated marine environment, carbon steel shows slight fluctuations in their E_{corr} values (± 50 mV). Variations in E_{corr} values were lower than those observed in the other environments, observing a slight tendency towards nobler potential towards the end of the test. However, these results show that in presence of chlorides and sulfates, the E_{corr} values of carbon steel are more active, indicating a low corrosion resistance.

In rural and marine environment, the initial drop in the E_{corr} values can be interpreted as an instability period associated with the corrosion of the material; subsequent behavior may be due to the formation of corrosion products onto carbon steel surface, wherein these corrosion products provide partial protection to the material [25].

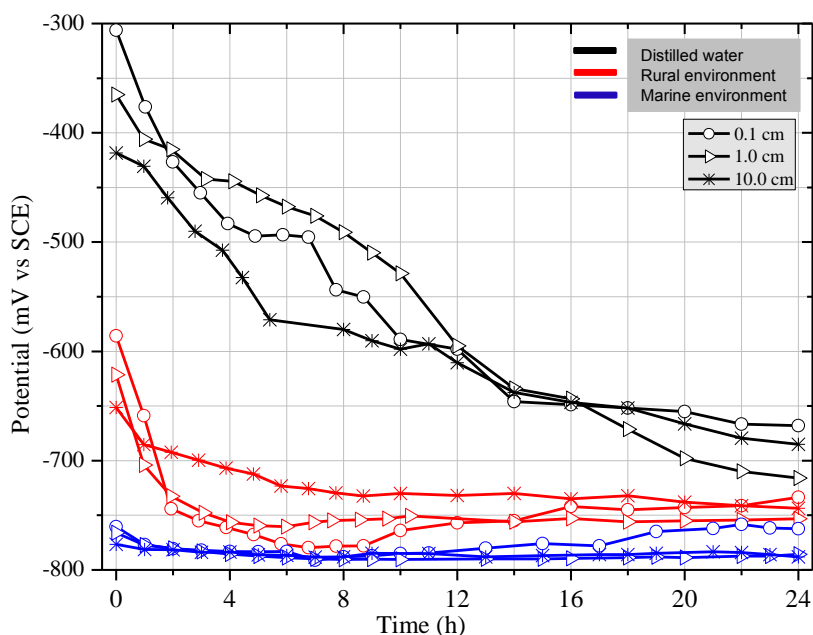


Figure 5. Variation in the E_{corr} values for carbon steel in simulated conditions of atmospheric corrosion.

3.3. Linear Polarization Resistance (LPR)

Figure 6 shows the effect of the depth of the solution layer on the polarization resistance for carbon steel evaluated in different environments.

In distilled water, regardless of the depth of the solution layer a rapid decrease in the R_p values in the first 8 hours of immersion was observed, subsequent for a depth of the solution layer of 0.1 cm the R_p values tend to increase, for a depth of the solution layer of 1.0 cm the R_p values remain almost constant, and for a depth of the solution layer of 10.0 cm the R_p values tend to increase. In general, these behaviors are associated with the amount of dissolved oxygen available, ie, the R_p values

increase by decreasing the depth of the solution layer [4, 17]. Similar behavior was observed in the Ecorr measurements.

In simulated rural environment, slight variations in the Rp values with a tendency to converge towards the end of the test are observed. In general, the Rp values are related to the depth of the solution layer, ie, for a lower depth of the solution layer, greater the Rp value. Similar behavior is observed in simulated marine environment, however the Rp values were lower. Again, LPR measurements show that in presence of chlorides and sulfates, the corrosion resistance of carbon steel was lower.

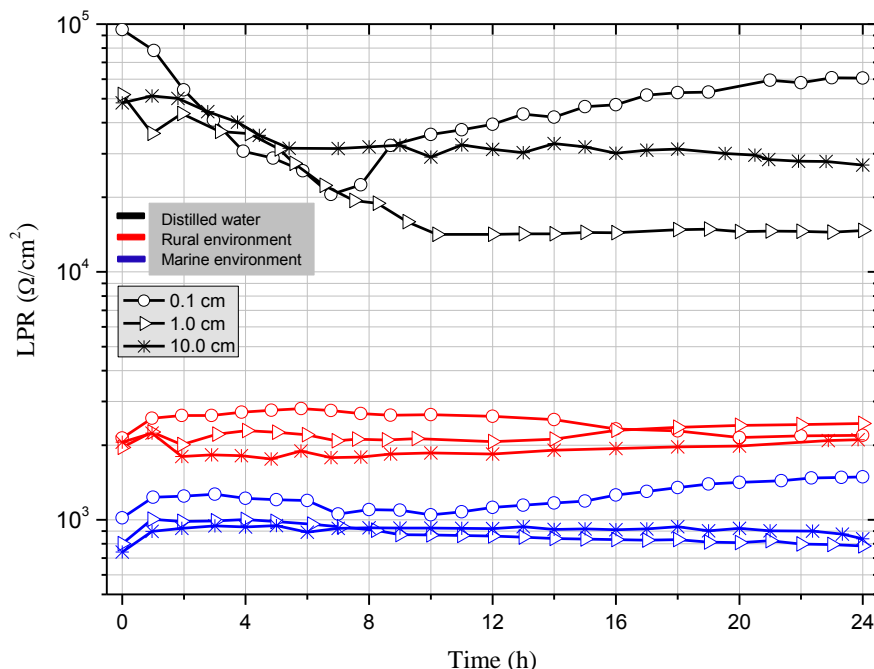


Figure 6. Variation in the polarization resistance for carbon steel in simulated conditions of atmospheric corrosion.

4. CONCLUSIONS

Potentiodynamic polarization curves, open circuit potential and linear polarization resistance measurements were realized in order to evaluate the effect of the depth of the solution layer on the corrosion process of carbon steel in different corrosive environments. In distilled water the polarization curves showed that by decreasing the depth of the solution layer, the Ecorr values become more active, and the cathodic current density decrease. This behavior is related to the amount of available oxygen into the solution layer. On the other hand, in rural environment was observed that by decreasing the depth of the solution layer, the Ecorr values become more active, but the cathodic limit current is the same. However, the length of the cathodic branch increases by increasing the depth of the solution layer. In marine environment was observed that by decreasing the depth of the solution layer, the Ecorr values become more active, and the cathodic current density was lower. Open circuit potential measurements showed drastic changes in the Ecorr values throughout the corrosion test. In

distilled water, Ecorr values tended steadily to more active values. This behavior is associated with a decrease in dissolved oxygen concentration available for the reduction reaction. In rural simulated environment, it was observed that regardless of the depth of the solution layer, Ecorr values tend around the same value. In marine environment, the variations in Ecorr values were lower than those observed in the other environments, observing a slight tendency towards nobler potential. From linear polarization resistance measurements, it was observed that in distilled water the Rp values increase by decreasing the depth of the solution layer, in rural environment the Rp values trend to converge towards the same value, and in marine environment the Rp values were lower.

ACKNOWLEDGEMENTS

Financial support from Consejo Nacional de Ciencia y Tecnología (CONACYT, México) (Projects 196205, 159898, and 159913) is gratefully acknowledged. Author M.E. Escalante-Perez is grateful for the grant given by CONACYT for his doctoral studies.

Conflict of Interests

The authors declare that there is no conflict of interests regarding the publication of this paper.

References

1. X. Liao, F. Cao, L. Zheng, W. Liu, A. Chen, J. Zhang, C. Cao, *Corros. Sci.*, 53 (2011) 3289-3298.
2. S.H. Zhang and S.B. Lyon, *Corros. Sci.*, 35 (1993) 713.
3. G.S. Frankel, M. Stratmann, M. Rohwerder, A. Michalik, B. Maier, J. Dora, M. Wicinski, *Corros. Sci.*, 49 (2007) 2021.
4. A. Nishikata, Y. Ichihara, Y. Hayashi, T. Tsuru, *J. Electrochemical Society*, 144 (1997) 1244.
5. N.D. Tomashov, *Corrosion*, 20(1964) 7t.
6. T. Tsuru, A. Nishikata, J. Wang, *Materials Science and Engineering*, A198 (1995) 161.
7. X. Fu, J. Dong, E. Han, W. Ke, *Sensors*, 9 (2009) 10400.
8. Kyung-Woo Chung, Kwang-Bum Kim, *Corros. Sci.*, 42 (2000) 517.
9. W. Liu, F. Cao, A. Chen, L. Chang, J. Zhang, Ch. Cao, *Corros. Sci.*, 52 (2010) 627.
10. M. Yamashita, H. Nagano, R.A. Oriani, *Corros. Sci.*, 39 (1998) 1447.
11. M.S. Venkatraman, I.G. Bosco, I.S. Cole, B. Emmanuel, *ECS Transactions*, 35 (2011) 1.
12. Y. Chen, D.M. Qi, H.P. Wang, Z. Xu, C.X. Yi, Z. Zhang, *Int. J. Electrochem. Sci.*, 10 (2015) 9056.
13. Z. Liu, W. Wang, J. Wang, X. Peng, Y. Wang, P. Zhang, H. Wang, C. Gao, *Corros. Sci.*, 80 (2014) 523.
14. Ch. Thee, L. Hao, J. Dong, X. Mu, X. Wei, X. Li, W. Ke, *Corros. Sci.*, 78 (2014) 130.
15. N.M. Markovic, T.J. Schmidt, V. Stamenkovic, P. N. Ross, *Fuel Cells*, 1 (2001) 105.
16. S. Hoerlé, F. Mazaudier, Ph. Dillmann, G. Santarini, *Corros. Sci.*, 46 (2004) 1431.
17. L. Cáceres, T. Vargas, L. Herrera, *Corros. Sci.*, 51 (2009) 971.
18. H. Huang, Z. Dong, Z. Chen, X. Guo, *Corros. Sci.*, 53 (2011) 1230.
19. S. Arzola, M.E. Palomar-Pardave, J. Genesca, *Journal of Applied Electrochemistry*, 33 (2003) 1223.
20. L. Fedrizzi, L. Ciaghi, P.L. Bonora, R. Fratesi, G. Roventi, *Journal of Applied Electrochemistry*, 22 (1992) 247.
21. C. Montesdeoca, J.J. Santana, F.J. Santana, J.E. González, *Información Tecnológica*, 12 (2001) 115.

22. S.H. Reiber, *Journal AWWA*, 81 (1989) 114.
23. Ching-Feng Lin, Kurt R. Hebert, *J. Electrochem. Soc.*, 141 (1994).
24. X.-P. Guo, Y. Tomoe, *Corrosion*, 54 (1998) 931.
25. El-Sayed M. Sherif, A.A. Almajid, A.K. Bairamov, Eissa Al-Zahrani, *Int. J. Electrochem. Sci.*, 6 (2011) 5430.

© 2016 The Authors. Published by ESG (www.electrochemsci.org). This article is an open access article distributed under the terms and conditions of the Creative Commons Attribution license (<http://creativecommons.org/licenses/by/4.0/>).